

SUPPORTING INFORMATION

Protective Mechanism of Dried Blood Spheroids: Stabilization of Labile Analytes in Whole Blood, Plasma, and Serum

Benjamin S. Frey,^a Deidre E. Damon,^a Danyelle M. Allen,^a Jill Baker,^a Sam Asamoah^a and Abraham K. Badu-Tawiah*

Supporting information is summarized below:

Table of Contents

	Description	Page
	<u>Experimental Methods</u>	3
	<u>Results and Discussion</u>	
	<i>Dried plasma and serum spot morphology</i>	
Fig. S1, S2	Dried plasma spot morphology on hydrophilic and hydrophobic paper substrate	4-5
Fig. S3, S4	Dried serum spot morphology on hydrophilic and hydrophobic paper substrate	6-7
	<i>Microscopic analysis of RBC morphology in whole blood deposited on hydrophilic and hydrophobic paper substrates</i>	
Fig. S5	SEM characterization of RBC morphology in DBS	8
Fig. S6	SEM characterization of RBC morphology in dried blood spheroids	9
	<i>Self-assembly and disintegration of RBCs at the exterior surface of dried blood spheroids</i>	
Fig. S7	SEM characterization of RBC self-assembly processes at the blood-air interface of dried blood spheroid	10
Fig. S8	SEM characterization of RBC disintegration at the blood-air interface of dried blood spheroids	11

Characterization of protective thin film thickness as a function of volume

Fig. S9 SEM characterization of the protective thin film of various volumes of dried blood spheroids 12

Impact of anticoagulants on the formation of the thin passivation layer in whole blood

Fig. S10 SEM characterization of whole blood from a K2-EDTA-capped tube compared to fresh whole blood from a finger stick 13

Potential anchoring mechanism of dried blood spheroids to hydrophobic paper

Fig. S11 SEM characterization of blood-paper interface of a dried blood spheroid 13

Thin film thickness of 3D-blood, -plasma, and -serum spots

Fig. S12 Thin film thickness of dried blood, plasma, and serum on hydrophobic paper substrate 14

Experimental Methods

Hydrophobic Paper Preparation. Precut filter paper was treated in a vacuum desiccator with 0.5 mL of trichloro(3,3,3-trifluoropropyl)silane. Untreated paper was not subject to this reaction. Paper triangles were 9.5 mm base × 16.6 mm height. Paper squares used in SEM were 10 mm base × 10 mm height. Whole blood samples were pipetted onto the paper surface and allowed to dry overnight unless otherwise stated.

Stability of Drugs in Biofluids. Cocaine was spiked into plasma and serum to final concentrations of 5 $\mu\text{g}/\text{mL}$, respectively. From these solutions, 20 ng of cocaine was deposited on the paper substrate. The samples were then dried and stored on a bench top under ambient conditions and analyzed via tandem mass spectrometry (MS/MS) by monitoring the signal (MS/MS transition m/z 304 \rightarrow 182) relative to its internal standard (MS/MS transition m/z 307 \rightarrow 185) for a minimum period of two weeks. Pure ethyl acetate containing 1 $\mu\text{g}/\text{mL}$ cocaine-d3 as the internal standard was used as the spray solvent for extraction processes. Samples were extracted with 20 μL aliquots of spray solvent.

Results and Discussion

Dried plasma spots on hydrophilic and hydrophobic paper substrate

Plasma (10 μL) was deposited onto the center of hydrophilic and hydrophobic squares and air-dried for 2 h. The samples were then imaged via compound light microscopy and scanning electron microscopy (Figure S1 and S2).

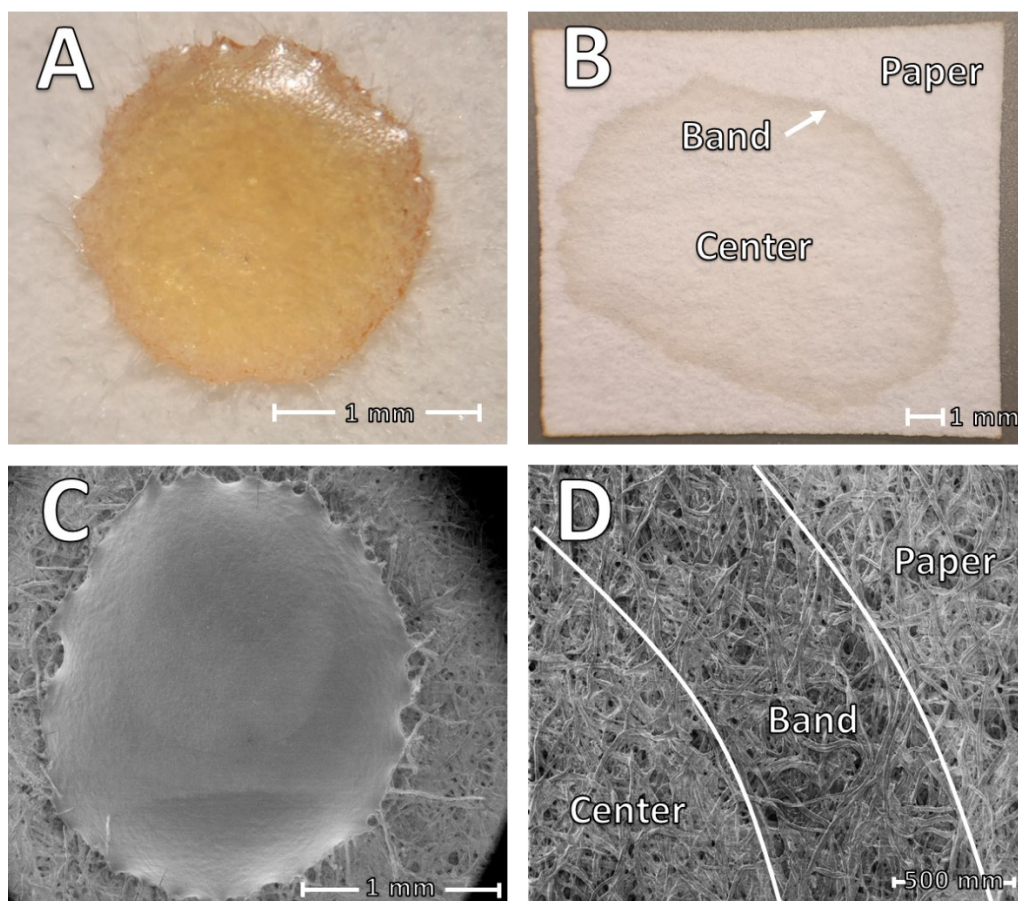


Figure S1. (A) Top-down compound light micrograph of a 10 μL 3D-plasma spot on hydrophobic paper substrate. (B) Top-down compound light micrograph of a 10 μL 2D-plasma spot on hydrophilic paper substrate. (C) Top-down scanning electron micrograph of a 10 μL 3D-plasma spot on hydrophobic paper substrate. (D) Top-down scanning electron micrograph of the peripheral edge (band region) of the 2D-plasma spot on hydrophilic paper substrate where the plasma forms a concentrated peripheral ring due to the coffee ring effect. Contrast has been increased 40% for this image for clarity.

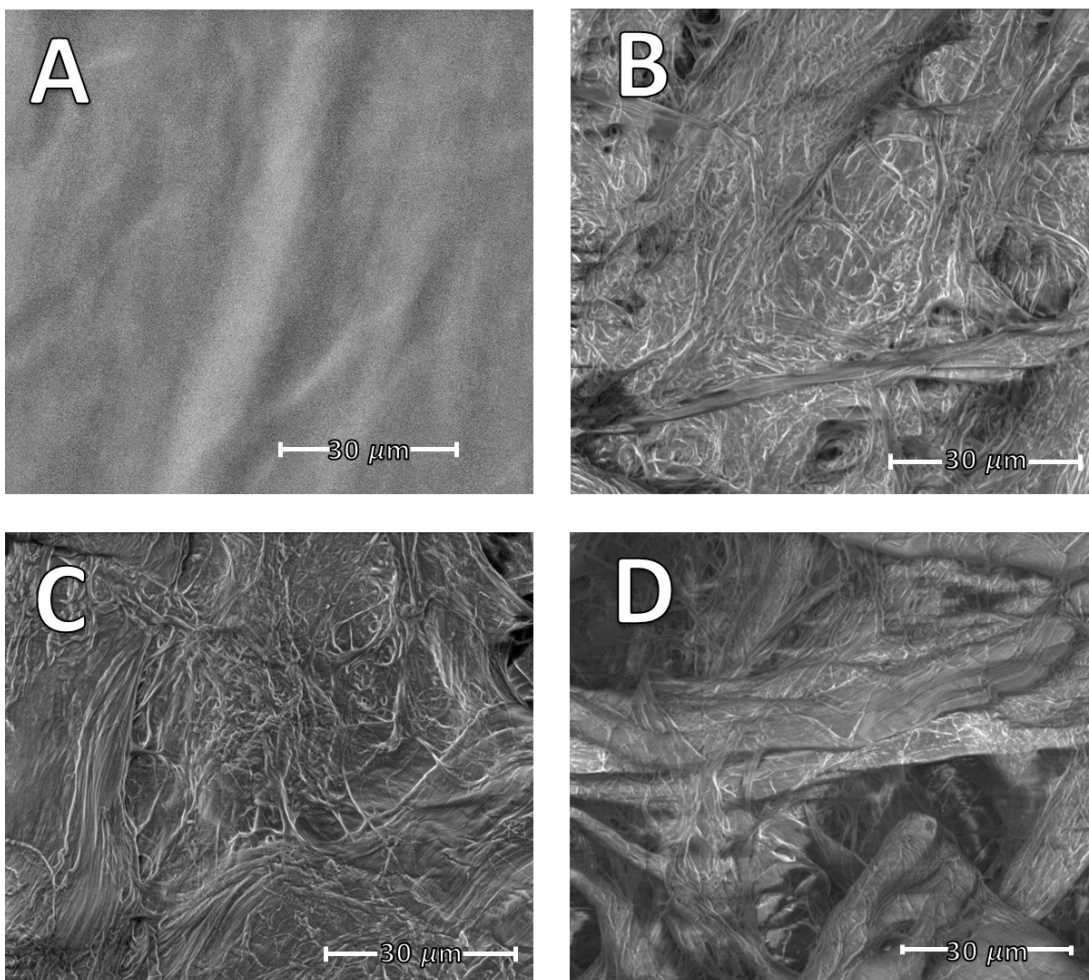


Figure S2. (A) Zoomed-in scanning electron micrograph of the exterior surface of a 10 μL 3D-plasma spot on hydrophobic paper substrate. (B) Zoomed-in scanning electron micrograph of the center region of a 10 μL 2D-plasma spot on hydrophilic paper substrate. (C) Zoomed-in scanning electron micrograph of the band region of a 10 μL 2D-plasma spot on hydrophilic paper substrate. Brightness has been enhanced by 20% for clarity. (D) Zoomed-in scanning electron micrograph of the paper region of the 2D-plasma spot on hydrophilic paper substrate.

Dried serum spots on hydrophilic and hydrophobic paper substrate

Serum (10 μL) was deposited onto the center of hydrophilic and hydrophobic squares and air-dried for 2 h. The samples were then imaged via compound light microscopy and scanning electron microscopy (Figure S3 and S4).

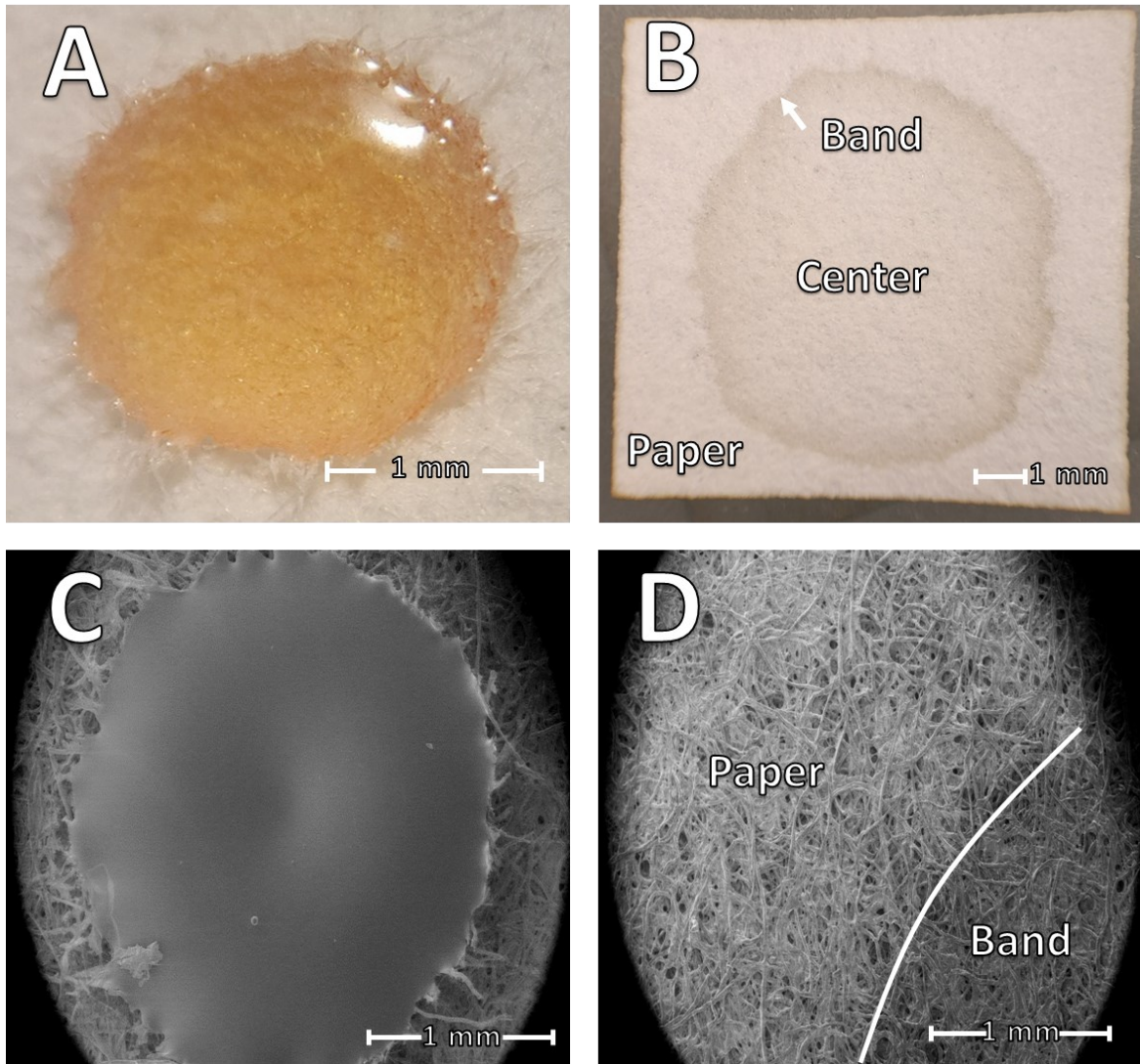


Figure S3. (A) Top-down compound light micrograph of a 10 μL 3D-serum spot on hydrophobic paper substrate. (B) Top-down compound light micrograph of a 10 μL 2D-serum spot on hydrophilic paper substrate. (C) Top-down scanning electron micrograph of a 10 μL 3D-serum spot on hydrophobic paper substrate. Brightness has been enhanced for this image by 40% for clarity. (D) Top-down scanning electron micrograph of the peripheral edge (band region)-paper interface of the 2D-serum spot on hydrophilic paper substrate where the serum forms a concentrated peripheral ring due to the coffee ring effect. Contrast has been enhanced for this image by 20% for clarity.

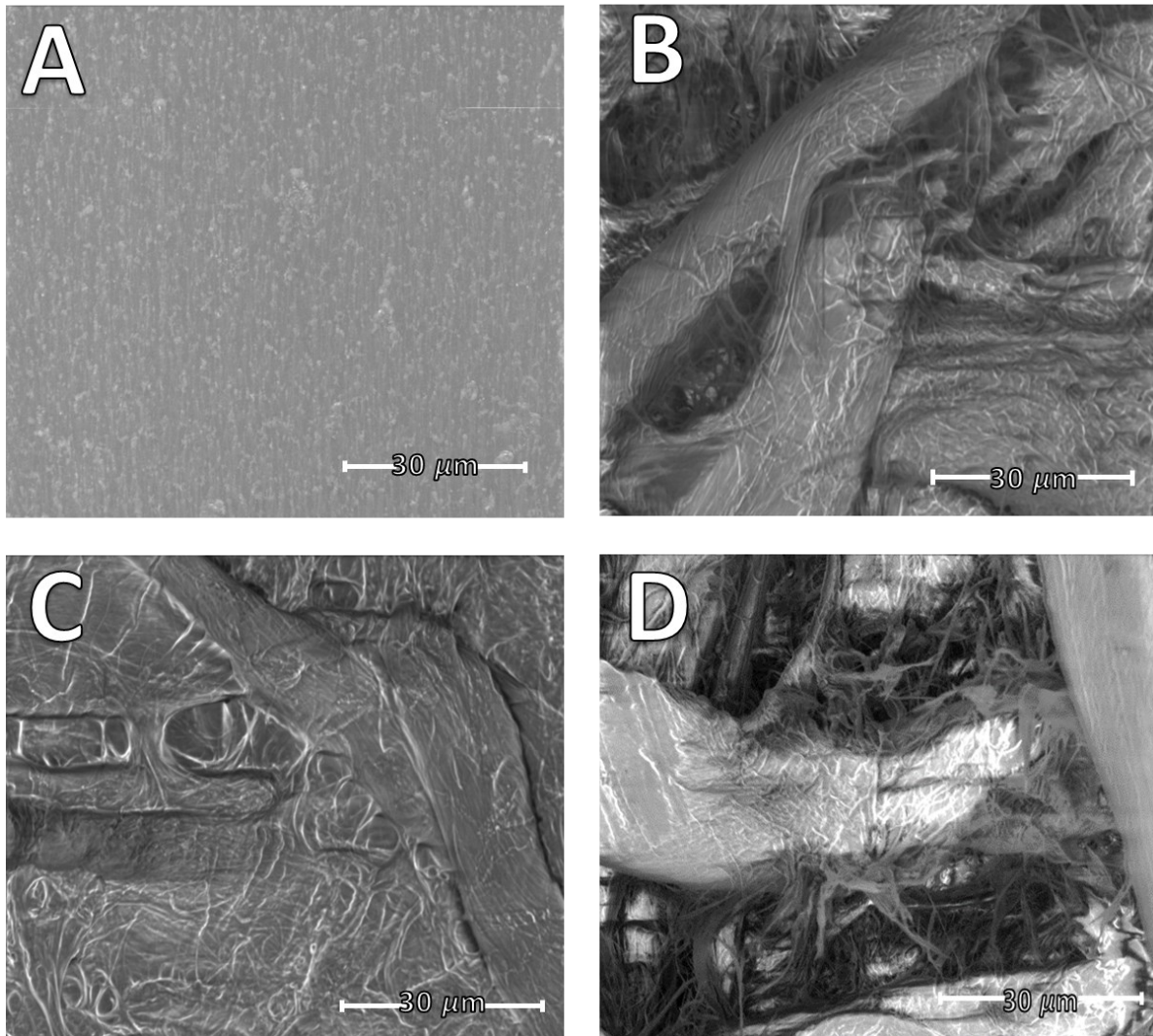


Figure S4. (A) Zoomed-in scanning electron micrograph of the exterior surface of a 10 μL 3D-serum spot on hydrophobic paper substrate. (B) Zoomed-in scanning electron micrograph of the center region of a 10 μL 2D-serum spot on hydrophilic paper substrate. (C) Zoomed-in scanning electron micrograph of the band region of a 10 μL 2D-serum spot on hydrophilic paper substrate. (D) Zoomed-in scanning electron micrograph of the paper region of the 2D-serum spot on hydrophilic paper substrate. Brightness has been enhanced for this image by 40% for clarity.

Microscopic analysis of RBC morphology on DBS and dried blood spheroids

Red blood cell morphology was first characterized for dried blood spots on hydrophilic paper substrate. Whole blood (10 μL) was deposited on the center of paper squares cut from Whatman grade 1 chromatography filter paper and was dried for the following amounts of time prior to fixation: 10 min, 1 h and 2 h. A FEI Nova 400 NanoSEM and FEI Quanta 200 SEM were used to collect images shown in Figure S5.

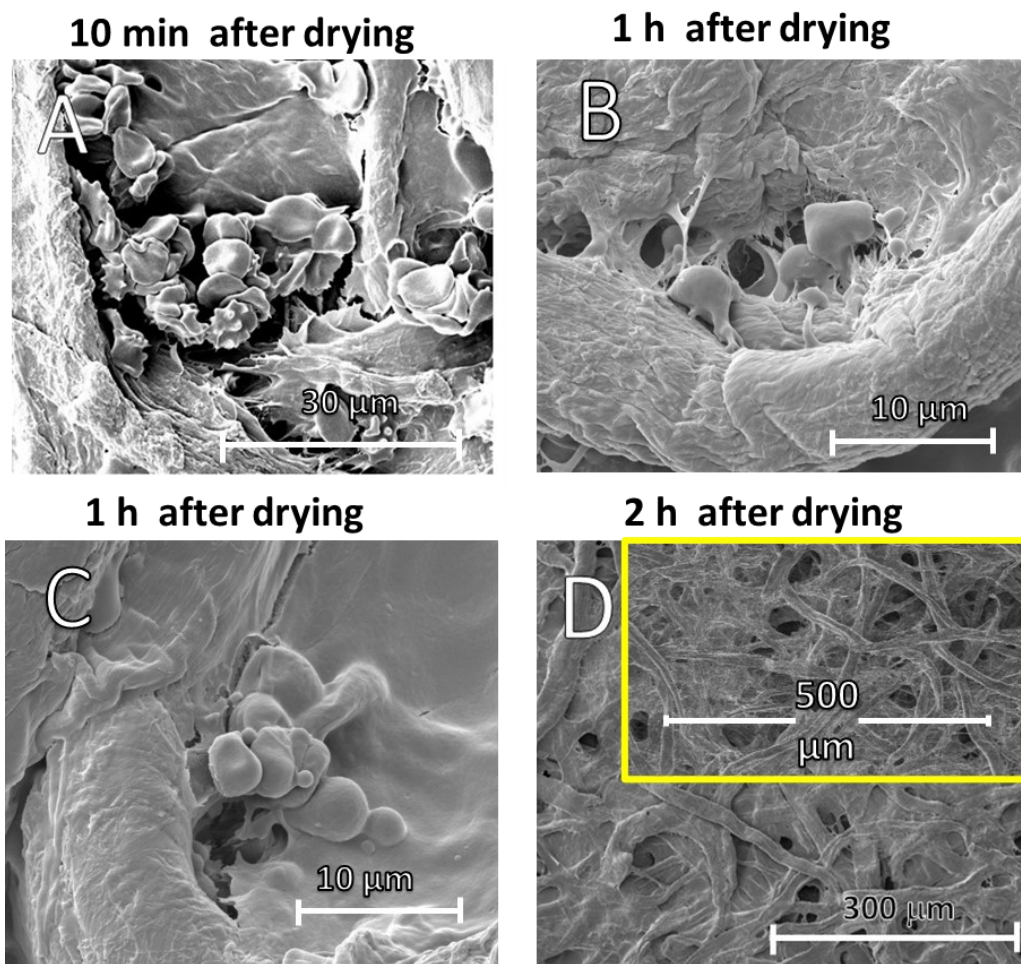


Figure S5. Dried blood spot dried samples derived from 10 μL whole blood was stored under ambient conditions for 10 min, 1 h and 2 h. Red blood cells absorb into the core of the paper substrate and rapidly begin to undergo hemolysis after sample deposition. (A) 10 min after drying, a few intact red blood cells remain. A conglomerate mass of red blood cells form within a pore of the paper substrate. (B) After 1 h drying, only a few red blood cells persist with partial disc morphology. Blood has begun fusing with the paper substrate. (C) 1 h after drying, red blood cells continue to undergo hemolysis and fuse with the paper substrate. (D) After 2 hours of storage under ambient condition, no distinguishable red blood cells with disc morphology are observed on the paper substrate. Inset in (D): chromatography filter paper without deposited blood sample.

Red blood cell morphology was then characterized on the exterior surface of dried blood spheroids. Dried blood spheroids form due to self-assembly processes of bio-macromolecules. To monitor changes in red blood cell morphology and formation of the spheroid, 10 μL of whole blood was deposited on the center of hydrophobic paper squares cut from Whatman grade 1 chromatography filter paper and was dried for the following amounts of time prior to fixation: 0 days, 1 day, 2 days, and 7 days. Samples were then allowed to dry overnight in ambient air and sputter coated with a thin layer of AuPd or Au. A FEI

Nova 400 NanoSEM and FEI Quanta 200 SEM were used to collect images. The exterior of the spheroids was analyzed as shown in Figure S6.

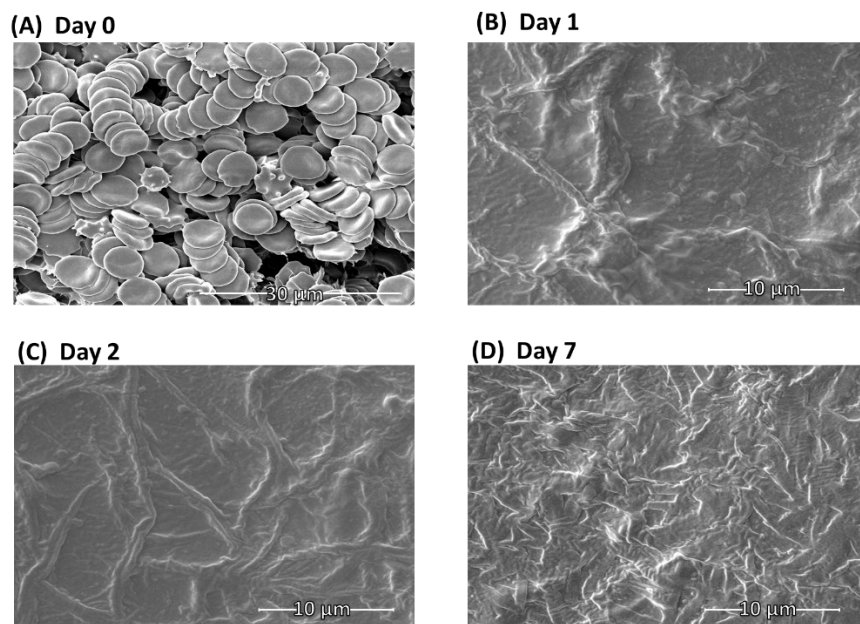


Figure S6. Characterization of exterior of red blood cells in a 10 μL dried blood spheroids. (a) After 1 h of drying under ambient conditions, intact, individual red blood cells are observed to be in rouleau conformation. (b) After 1 day of storage under ambient conditions, no traces of red blood cells exist. The red blood cells have all undergone hemolysis and have fused together. The fibrous-like structures may be fibrin molecules that have become concentrated during self-assembly processes. (c) The fibrous-like structures appear to be finer in structure, likely due to on-going coagulation processes. No red blood cells are observed. (d) After 7 days of storage, there are many tiny hair-like structures that are believed to be fibrin and other clotting proteins.

Characterization of the self-assembly and disintegration processes of red blood cells on the exterior surface of dried blood spheroids

To characterize the self-assembly and disintegration processes of red blood cells on the exterior surface of dried blood spheroids, whole blood (10 μL) was deposited on the center of hydrophobic paper squares cut from Whatman grade 1 chromatography filter paper and was dried under ambient conditions for at least 0.5 h prior to being fixed in a 2.5% glutaraldehyde solution buffered to pH 7.4 with 0.1 M phosphate buffer. Fixed samples were dried overnight in ambient air and sputter coated with a thin layer of AuPd or Au. An FEI Quanta 200 SEM was used to collect images of the exterior of the dried blood spheroids as shown below.

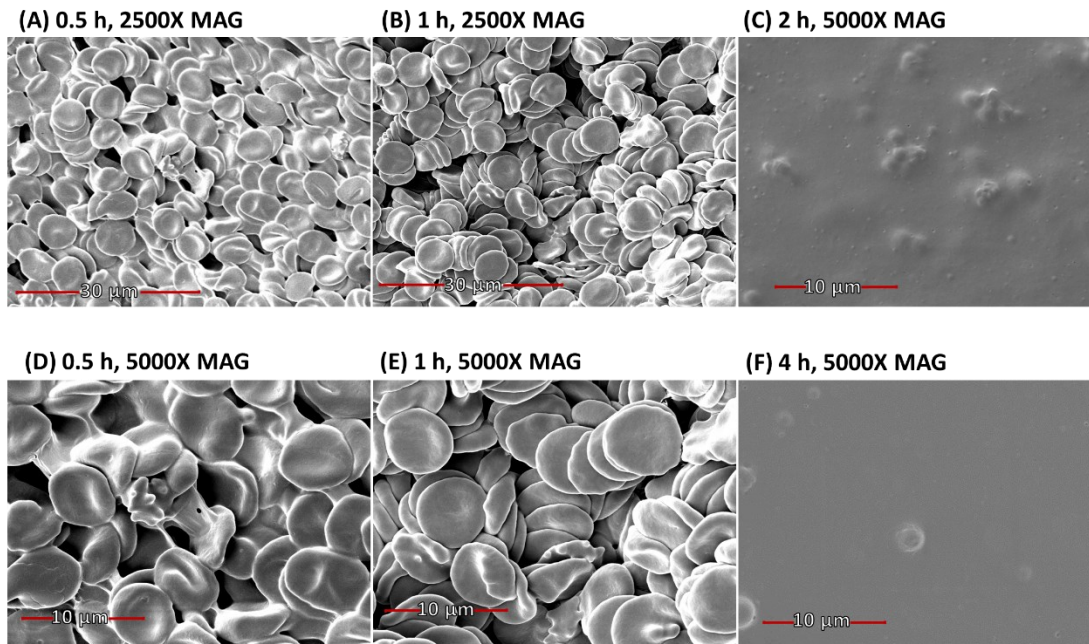
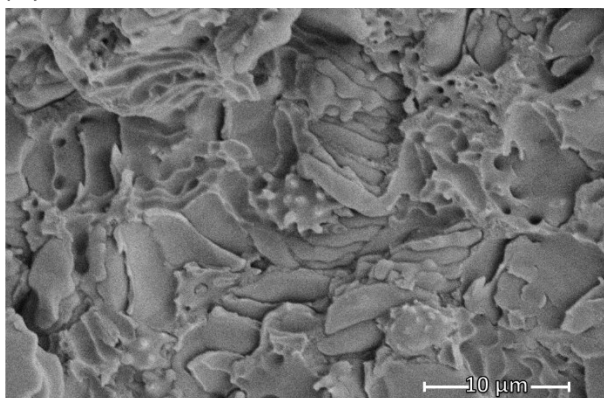


Figure S7. SEM characterization of self-assembly of red blood cells on exterior surface of a 10 μ L dried blood spheroids. (A) Panned out micrograph (2500X MAG) of the exterior surface of a dried blood spheroid after drying under ambient conditions for 0.5 h. (B) Panned out micrograph (2500X MAG) of the exterior surface of a dried blood spheroid after drying under ambient conditions for 1 h. Red blood cells begin to form rouleau and begin to coagulate together. (C) Micrograph of the exterior surface of a dried blood spheroid after drying under ambient conditions for 2 h. Tiny remnants of individual red blood cells exist; red blood cells have largely undergone hemolysis and fusion to form the outer protective barrier. (D) Zoomed-in (5000X MAG) of the exterior surface of a dried blood spheroid shown in (A). Bridging of red blood cells occurs, likely due to fibrin also migrating to the outer peripheral region of the spheroid during solvent evaporation. (E) Zoomed-in micrograph (5000X MAG) of the exterior surface of a dried blood spheroid shown in (B). Stacks of red blood cells in the form of rouleau exist with close association between each red blood cell. (F) Micrograph of the exterior surface of a dried blood spheroid dried for 4 h. Almost all red blood cells have undergone hemolysis on the outer surface, with very few remaining in-tact red blood cells.

(A) 80 min



(B) 100 min

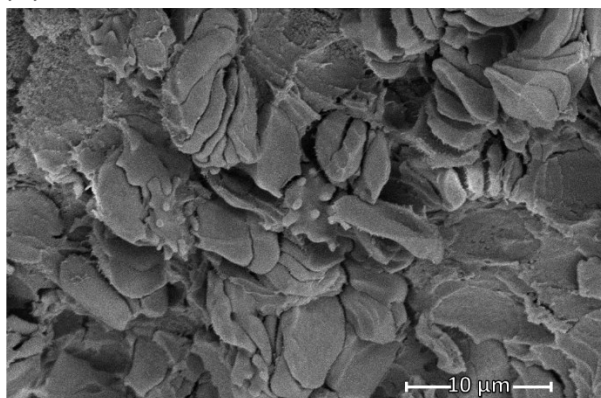


Figure S8. (A) Exterior surface of a 10 μL dried blood spheroid after drying under ambient storage conditions for 80 m. Spiney-like red blood cells undergoing hemolysis and fusion are observed, as well as the disintegration of rouleau as the hemolysis process occurs. Destroyed red blood cells have a spongy coral-like appearance. (B) Exterior surface of a 10 μL dried blood spheroid after drying under ambient storage conditions for 100 m. Continued destruction, hemolysis, and unpacking of rouleau conformation as the outer protective barrier forms.

Characterizing the thin protective barrier thickness as a function of sample volume

The thickness of the outer protective barrier was measured as a function of the initial sample volume of the dried blood spheroid (Figure S5). To investigate the protective barrier thickness, 4, 10, 25 and 50 μL of whole blood was deposited onto the center of hydrophobic paper squares cut from Whatman grade 1 chromatography filter paper and was dried under ambient conditions for at least 4 h prior to being fixed in a 2.5% glutaraldehyde solution buffered to pH 7.4 with 0.1 M phosphate buffer. Samples were then allowed to dry overnight in ambient air. These samples were analyzed without any metal coating at room temperature with a water vapor pressure of 50 Pa in the chamber.

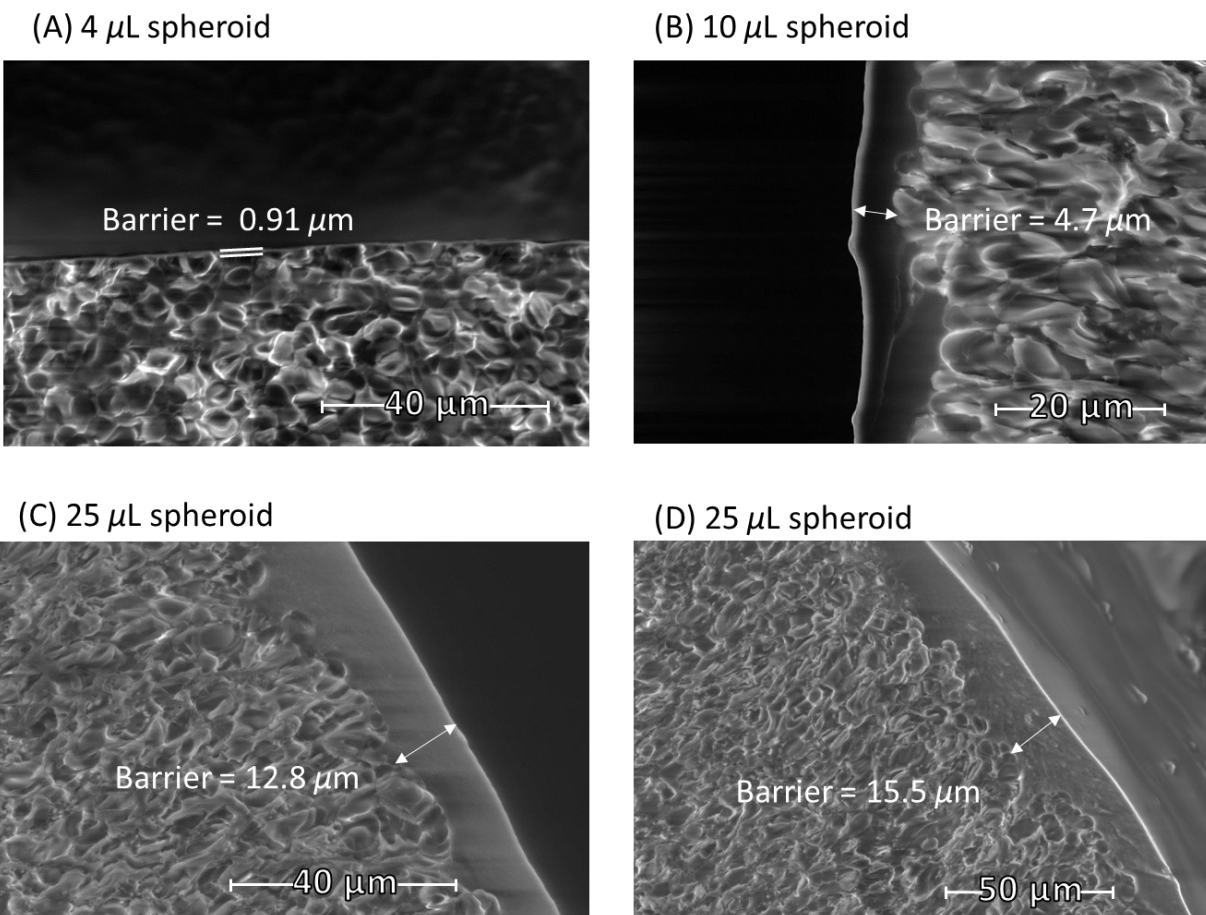
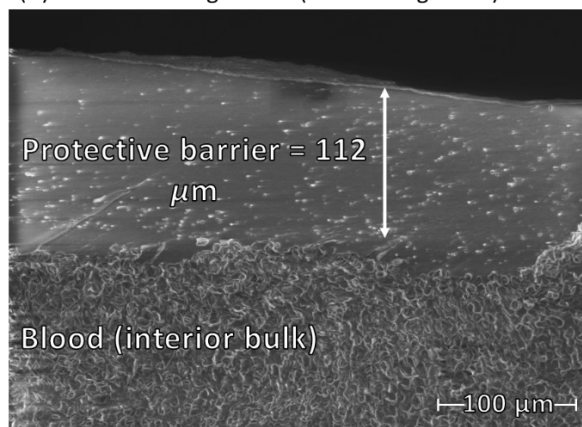


Figure S9. Differences in thickness of thin protective barriers found in cross sections of (A) 4 μL dried blood spheroids, (B) 10 μL dried blood spheroids, (C) 25 μL dried blood spheroids, and (D) 50 μL dried blood spheroids. All samples were dried under similar conditions (e.g., temperature, humidity) for the same amount of time (4 h). The thickness of the protect barrier ranged from 0.91, 4.7, 12.8, and 15.5 μm for blood volumes 4, 10, 25, and 50 μL respectively. Image brightness was enhanced by 20% for clarity.

Impact of anticoagulants on the formation of the thin passivation layer in whole blood

Whole blood (10 μL) from a finger stick and K2-EDTA-capped tube were deposited on hydrophobic paper squares and were air-dried for 2 h. The cross section of the two dried blood spheroids were then imaged via scanning electron microscopy. The presence of anticoagulants (ethylenediaminetetraacetic acid) reduces intermolecular interactions between adjacent red blood cells and clotting factors, therefore reducing the thickness of the barrier. A visible barrier of approximately 112 μm was observed for blood obtained from a finger stick while a barrier of approximately 10.5 μm was observed for blood obtained from a collection tube containing anticoagulant.

(A) Blood from Finger Stick (no anticoagulants)



(B) Blood from K2-EDTA-capped tubes (anticoagulant present)

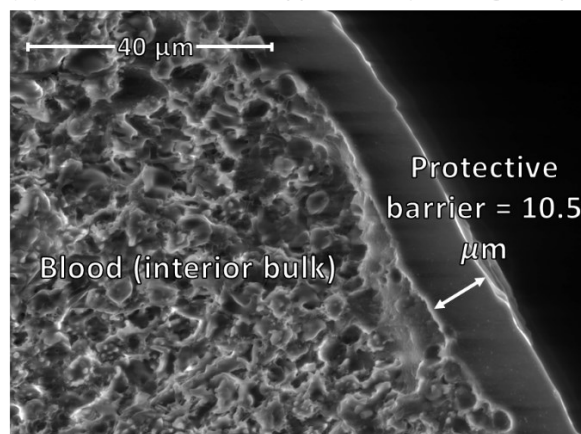


Figure S10. Comparison of thickness of the protective barrier in dried blood spheroids with and without anticoagulants. (A) Blood obtained directly from a finger stick without anticoagulants. (B) Blood obtained from a K2-EDTA-capped collection tube with anticoagulants. Image brightness and contrast for (B) was enhanced by 20% for clarity.

Potential anchoring mechanism of dried blood spheroids to hydrophobic paper substrate

Whole blood (10 μL) was deposited onto hydrophobic paper substrate and was dried for 1 h. The dried blood spheroid was then imaged via scanning electron microscopy. Prior to microscopic analysis, the dried blood spheroid underwent delamination processes to separate the blood-paper interface. The bottom portion of the dried blood spheroid was then imaged.

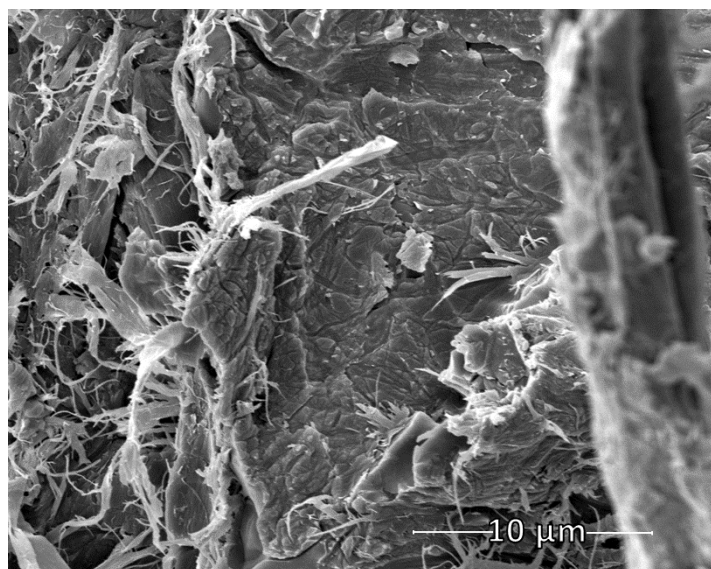


Figure S11. Evidence of anchoring of a dried blood spheroid to paper substrate by interaction with fibrin at the blood-paper interface. The dried blood spheroid was gently lifted from one edge using forceps to expose the blood-paper interface.

Thin film thickness of dried blood, plasma, and serum on hydrophobic paper substrate

Whole blood, plasma, and serum ($10 \mu\text{L}$) were deposited onto the center of hydrophobic squares and air-dried for 2 h. The cross section of each sample was imaged via scanning electron microscopy. Whole blood had the largest film thickness due to the presence of red blood cells, which has a thickness of approximately $896 \mu\text{m}$ from the base of the paper substrate to the apex of the dried blood spheroid. Plasma had the next largest film thickness of approximately $390 \mu\text{m}$ while serum had a film thickness of $350 \mu\text{m}$. The differences in film thickness can be attributed to the presence or absence of biomacromolecules (e.g., red blood cells, clotting factors, etc.).

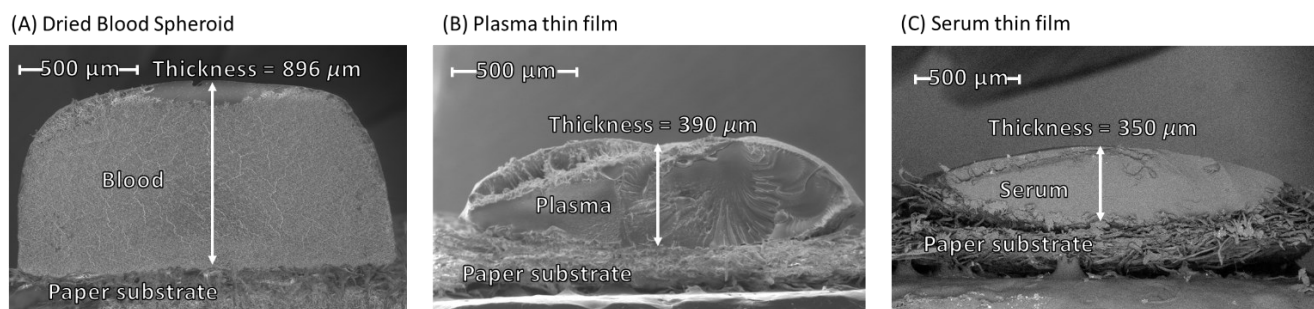


Figure S12. Cross-sectional thin film thickness of $10 \mu\text{L}$ (A) whole blood, (B) plasma, and (C) serum spotted onto hydrophobic paper substrate.